



Distinct pattern of hypometabolism and atrophy in preclinical and prodementia Alzheimer's disease



Vanja Kljajevic^{a,*}, Michel Jan Grothe^{a,1}, Michael Ewers^b, Stefan Teipel^{a,c}, for the Alzheimer's Disease Neuroimaging Initiative²

^a German Center for Neurodegenerative Diseases (DZNE), Rostock, Germany

^b Institute for Stroke and Dementia Research (ISD), Klinikum Grosshadern, Ludwig-Maximilians University, Munich, Germany

^c Department of Psychosomatics and Psychotherapeutic Medicine, University of Rostock, Rostock, Germany

ARTICLE INFO

Article history:

Received 20 September 2013

Received in revised form 1 April 2014

Accepted 5 April 2014

Available online 13 April 2014

Keywords:

Alzheimer's disease

Amyloid

Imaging biomarkers

Mild cognitive impairment

ABSTRACT

The goal of the present study was to determine the earliest patterns of hypometabolism and atrophy in the development of Alzheimer's disease (AD). Stages of AD were defined by positron emission tomography imaging evidence of cortical amyloid pathology in addition to cognitive criteria. Subjects for the study were selected from the Alzheimer's Disease Neuroimaging Initiative database and divided into 4 groups: cognitively normal (CN) amyloid negative ($A\beta^-$) elderly subjects ($n = 36$), CN amyloid-positive ($A\beta^+$) ($n = 21$), early mild cognitive impairment $A\beta^+$ ($n = 65$), and late mild cognitive impairment $A\beta^+$ ($n = 23$) subjects. Region of interest-based (primary) and voxel-based (secondary) analyses were used to assess gray matter hypometabolism, quantified by [^{18}F]fluorodeoxyglucose-positron emission tomography, and decrease in gray matter volume and cortical thickness was measured by magnetic resonance imaging. Region of interest- and voxel-based analyses showed significant hypometabolism but not atrophy in CN $A\beta^+$ subjects compared with CN $A\beta^-$ subjects. The results suggest that hypometabolism exceeds atrophy in preclinical AD, supporting the notion that amyloid load may affect synaptic activity, leading to synaptic loss and subsequent neuronal loss.

© 2014 Elsevier Inc. All rights reserved.

1. Introduction

The amyloid cascade hypothesis assumes that the deposition of beta-amyloid (β -amyloid) peptides, derived from amyloid precursor protein, in brain parenchyma is the main cause of a pathologic sequence of events leading to neuronal loss and dementia in Alzheimer's disease (AD) (Glenner and Wong, 1984; Hardy and Allsop, 1991; Karran et al., 2011; Pimplikar, 2009). While β -amyloid is a normal product of neuronal cells and is found in the cerebrospinal fluid (CSF) and plasma, the processing of amyloid precursor protein in AD is disturbed: the imbalance between β -amyloid production and clearance leads to amyloid accumulation, which may trigger

processes that lead to the disease (Hardy and Higgins, 1992). Some researchers have challenged the amyloid cascade hypothesis (Castellani and Smith, 2011), arguing that, on the contrary, β -amyloid may have a protective role in the disease and that its increase reflects a response to the disease, not its cause (Lee et al., 2004). Nevertheless, increased β -amyloid in the brain has been associated with the disruption of synaptic connections and neuronal death in dementia (Hardy and Allsop, 1991).

Unlike neurofibrillary tangles of misfolded tau-protein, another key neuropathological feature of AD, β -amyloid plaques show only weak association to neuronal loss or dementia severity and do not correlate with the disease duration (Karran et al., 2011). Thus, β -amyloid aggregation and deposition may facilitate tau pathology, triggering a cascade of events that mediate neuronal loss. Synaptic dysfunction, which accompanies neurodegeneration in AD, is reflected in striking hypometabolic alterations imaged by [^{18}F]fluorodeoxyglucose positron emission tomography (FDG-PET) and precedes dementia symptoms in subjects who eventually progress to AD (Chetelat et al., 2008; Mosconi, 2005).

Recently redefined research and diagnostic criteria for Alzheimer's disease (Albert et al., 2011; Dubois et al., 2007, 2010; Sperling et al., 2011) have promoted a concept of AD as a

* Corresponding author at: German Center for Neurodegenerative Diseases (DZNE), Gehlsheimer Straße 20, D- 18147 Rostock, Germany. Tel.: +49 381 494 9628; fax: +49 381 494 9472.

E-mail address: vanja.kljajevic@dzne.de (V. Kljajevic).

¹ These authors contributed equally to this work.

² Data used in preparation of this article were obtained from the Alzheimer's Disease Neuroimaging Initiative (ADNI) database (adni.loni.ucla.edu). As such, the investigators within the ADNI contributed to the design and implementation of ADNI and/or provided data but did not participate in analysis or writing of this report. A complete listing of ADNI investigators can be found at: http://adni.loni.ucla.edu/wp-content/uploads/how_to_apply/ADNI_Acknowledgement_List.pdf.

continuum including preclinical, predementia, and dementia stages strongly emphasizing the role of biomarkers in identifying stages of the disease (Jagust et al., 2009; Khachaturian et al., 2012; Ossenkoppele et al., 2011). Crucially, as the disease progresses, its stages seem to be possible to map to specific AD biomarkers that appear in a certain temporal order (Jack et al., 2010, 2013). Currently, the most validated AD biomarkers include amyloid β_{42} , total tau, and phospho-tau as pathophysiological markers, and hypometabolism and gray matter (GM) atrophy as topographical markers (Dubois et al., 2010). It has been proposed that hypometabolism precedes GM atrophy and that the 2 markers have different anatomic origins in the AD brain (Jack et al., 2010). Furthermore, evidence from autosomal dominant AD, on which sporadic AD is typically modeled, also shows that cortical hypometabolism appears before cortical atrophy (Benzinger et al., 2013; Mosconi et al., 2006).

Only a small number of studies assessed hypometabolic and atrophic patterns in asymptomatic sporadic AD as defined by cognitively normal (CN) subjects with increased PET-measured amyloid load (amyloid-positive, $A\beta+$) (Sperling et al., 2011). One study reported no significant metabolic differences between CN $A\beta+$ and CN amyloid-negative ($A\beta-$) control subjects, and atrophic patterns were not assessed (Cohen et al., 2009). By contrast, another study reported significant posterior cingulate cortex hypometabolism in CN $A\beta+$ subjects compared with CN $A\beta-$ subjects, but no significant GM reductions in AD susceptible areas (Drzezga et al., 2011). However, the sample size of this study was rather small (12 CN $A\beta-$, 12 CN $A\beta+$).

The limited and partially discordant data regarding the relative contributions of atrophy and hypometabolism in (biomarker-verified) preclinical and predementia stages of sporadic AD have demanded a more thorough assessment of these *in vivo* changes. To meet this demand, in the present study we included relatively large groups and in addition to assessing hypometabolism we also assessed atrophy by means of 2 widely used complementary techniques (GM volume and cortical thickness), as well as region of interest (ROI)- and voxel-based analyses.

The main goal of the present study was to determine whether hypometabolism exceeds atrophy in sporadic AD, focusing on the earliest point of disease development. Because deposited β -amyloid appears to be a necessary condition for the eventual development of AD dementia (Buchhave et al., 2012; Nordberg et al., 2013), in the present study we characterized asymptomatic and predementia stages of AD by the presence of significant cortical β -amyloid load, as assessed by AV45-PET imaging, in addition to cognitive criteria (Albert et al., 2011; Sperling et al., 2011). Structural magnetic resonance imaging (MRI) and FDG-PET were then used to investigate patterns of hypometabolism and GM atrophy in asymptomatic and predementia stages of AD as compared with cognitively normal subjects without signs of pathology on amyloid-PET imaging. If hypometabolism precedes atrophy in the development of AD, one would expect to find significant hypometabolism in asymptomatic stages of AD at which atrophy is not yet significant.

2. Methods

2.1. Data source

Data used in the preparation of this article were obtained from the ADNI database (adni.loni.ucla.edu). The ADNI was launched in 2003 by the National Institute on Aging, the National Institute of Biomedical Imaging and Bioengineering, the Food and Drug Administration, private pharmaceutical companies and nonprofit organizations, with the primary goal to test whether serial MRI, PET, other biological markers, and clinical and neuropsychological

assessment can be combined to measure the progression of mild cognitive impairment (MCI) and early AD. A fuller description of ADNI is given in the [Supplementary Material](#) and up-to-date information is available at www.adni-info.org.

2.2. Subjects

AV45-PET, FDG-PET, and structural MRI data of 245 individuals were originally retrieved from the ADNI-GO and ADNI-2 extensions of the ADNI project. They included imaging data of 57 cognitively normal (CN) elderly subjects, 156 subjects at an early stage of mild cognitive impairment (EMCI), and 32 subjects at a more advanced (“late”) stage of mild cognitive impairment (LMCI). Detailed inclusion criteria for the diagnostic categories can be found at the ADNI web site (<http://www.adni-info.org/Scientists/AboutADNI.aspx>). Briefly, CN subjects have Mini Mental State Examination (MMSE) scores between 24 and 30 (inclusive), a Clinical Dementia Rating score of 0 are nondepressed, non-MCI, and nondemented. EMCI subjects have MMSE scores between 24 and 30 (inclusive), a subjective memory concern reported by subject, informant, or clinician, objective memory loss measured by education adjusted scores on delayed recall (one paragraph from Wechsler Memory Scale Logical Memory II; education adjusted scores: ≥ 16 years: 9–11; 8–15 years: 5–9; 0–7 years: 3–6), a Clinical Dementia Rating of 0.5, the absence of significant levels of impairment in other cognitive domains, essentially preserved activities of daily living, and the absence of dementia. Diagnosis of LMCI differs from that of EMCI only in a higher degree of objective memory impairment (education adjusted scores: ≥ 16 years: ≤ 8 ; 8–15 years: ≤ 4 ; 0–7 years: ≤ 2).

Diagnostic groups were dichotomized into $A\beta+$ and $A\beta-$ subgroups, based on a cutoff of 1.28 cortex-to-cerebellar GM AV45 uptake value ratio (see Section 2.4.1). Amyloid-negative MCI subjects were omitted from analyses, which resulted in a sample of 145 subjects: 36 CN $A\beta-$ subjects representing the control group, and 21 CN $A\beta+$, 65 EMCI $A\beta+$, and 23 LMCI $A\beta+$ subjects representing asymptomatic and predementia AD groups, respectively.

Data for the present study were downloaded in November, 2011. We checked for possible changes in diagnostic status of subjects in each study group in December, 2013. All but 2 EMCI subjects in our sample have had a record of follow up visits, with an average number of days between the first and the last visit of 729 days for the EMCI group, 714 for the LMCI group, 734 days for CN $A\beta+$ subjects, and 710 for CN $A\beta-$ subjects. In the EMCI group, there were 58/63 (92.1%) subjects with stable MCI status, 4 cases of conversion to AD, and 1 case of reversion to normal status. The LMCI group had only 9/23 (39.1%) stable MCI cases and 14 cases (60.9%) of conversion to AD. The group of CN $A\beta+$ subjects was stable with 18/21 (85.7%) of subjects with unchanged status and 3 MCI converters. In the CN $A\beta-$ group, there were 34/36 (94.4%) subjects with unchanged diagnostic status, 1 case of conversion to MCI and 1 case of conversion to AD.

2.3. Imaging data acquisition

ADNI-GO/-2 MRI data were acquired on multiple 3T MRI scanners using scanner-specific T1-weighted sagittal 3D MPRAGE sequences. To increase signal uniformity across the multicenter scanner platforms, original MPRAGE acquisitions in ADNI undergo standardized image preprocessing correction steps. AV45 and FDG-PET data were acquired on multiple instruments of varying resolution and following different platform-specific acquisition protocols. Similar to the MRI data, PET data in ADNI undergo standardized image preprocessing correction steps aimed at increasing data uniformity across the multicenter acquisitions. More detailed information on the different imaging protocols used across ADNI sites and

standardized image preprocessing steps for MRI and PET acquisitions can be found in the [Supplementary Material](#) and at the ADNI web site (<http://adni.loni.usc.edu/methods/>).

2.4. Imaging data processing

2.4.1. AV45-PET data processing

Cortical AV45 standardized uptake value ratios (SUVR) relative to cerebellar GM uptake were calculated by one of the ADNI PET core laboratories and are available on the ADNI server. Based on an image-processing stream using FreeSurfer software (version 4.5.0), a composite cortical AV45 SUVR for each subject was derived from the average uptake within cortical summary regions divided by the uptake of a cerebellar reference region. For establishing amyloid positivity or negativity based on the composite cortical AV45 SUVR, a cutoff of 1.28 has been recommended. This cutoff is extrapolated from a previously validated PiB-PET SUVR cutoff of 1.47, by combined assessment of PiB- and AV45-PET in 21 ADNI subjects who underwent both types of amyloid-PET scanning. These methods are described in greater detail by the group ([Jagust et al., 2009; Mormino et al., 2009](#)) and on the ADNI web site (<http://adni.loni.usc.edu/methods/pet-analysis/>).

2.4.2. MRI volumetric data processing

Imaging data were processed using Statistical Parametric Mapping (SPM8, Wellcome Trust Center for Neuroimaging) and the VBM8-toolbox (<http://dbm.neuro.uni-jena.de/vbm/>) implemented in MATLAB R2007a (MathWorks, Natick, MA, USA). First, MRI scans were automatically segmented into GM, white matter (WM), and CSF partitions of 1.5 mm isotropic voxel-size, using the tissue prior free segmentation routine of the VBM8-toolbox. The resulting GM and WM partitions of each subject in native space were then high-dimensionally registered to an aging and/or AD-specific reference template from a previous study ([Grothe et al., 2013](#)) using DARTEL ([Ashburner, 2007](#)). Individual flow-fields obtained from the DARTEL registration to the reference template were used to warp the GM segments and voxel-values were modulated for volumetric changes introduced by the high-dimensional normalization, such that the total amount of GM volume present before warping was preserved. Finally, modulated warped GM segments were smoothed with a Gaussian smoothing kernel of 8 mm full-width at half maximum.

2.4.3. MRI cortical thickness data processing

Since cortical thinning is another potential imaging marker for atrophic changes in AD ([Dickerson et al., 2009](#)), we computed thickness of the cortical GM using FreeSurfer 5.1 software (<http://surfer.nmr.mgh.harvard.edu/>) ([Dale et al., 1999; Fischl et al., 1999](#)). The preprocessing steps followed the recommendations available on the FreeSurfer web site (<http://surfer.nmr.mgh.harvard.edu/fswiki/FreeSurferAnalysisPipelineOverview>) and included: linear registration of the MPRAGE scans with MNI (Montreal Neurological Institute) standard space, skull-stripping, segmentation of brain matter into GM, WM, and CSF, extraction of the inner and outer cortical surfaces, and flattening of the brain. The resulting surface maps were visually inspected and in cases where the preprocessing did not produce a high quality result, producing for instance incorrect boundaries, inaccurate spatial registration, or other defects, the next step was to apply corrections and then re-run preprocessing for that particular subject. Finally, the distance between the gray/white boundary to the gray/CSF boundary was used to calculate cortical thickness estimates at each vertex.

2.4.4. FDG-PET data processing

Each subject's FDG-PET scan was rigidly coregistered to the corresponding structural MRI scan. After visual confirmation of

successful alignment to the MRI scan, FDG-PET scans were warped to the aging/AD-specific reference space (without modulation of voxel-values) using the DARTEL flow-fields derived from the registration of the MRI scans. Finally, warped FDG-PET scans were multiplied with a binary GM mask of the aging/AD template, thresholded at 20% GM probability, and subsequently smoothed with a Gaussian smoothing kernel of 8 mm full-width at half maximum.

2.4.5. Definition of ROIs

Two sets of predefined ROIs—"metabolic" (i.e., FDG-PET-based) and "structural" (MRI-based) were derived from a previous study assessing voxel-wise patterns of FDG-PET hypometabolism and GM atrophy in an independent data set, consisting of 78 CSF-A β -positive MCI subjects and 30 CSF-A β -negative cognitively normal subjects from ADNI-1 ([Ewers et al., 2013](#)). Statistical maps of hypometabolism and GM atrophy were thresholded at $p < 0.05$, FDR-corrected, and warped to the reference space of the aging/AD-specific template of this study using DARTEL. Clusters in the left and right inferior parietal areas and medial parietal region were used to define metabolic ROIs, whereas clusters in the left and right lateral temporal areas, and left and right medial temporal lobe areas served as targets in the definition of the structural volumetric ROIs. In addition to gray matter density, we also tested for cortical thickness differences, because we wanted to be as sensitive as possible for atrophy effects. To this end, a set of cortical thickness ROIs was derived from the Desikan anatomic atlas ([Desikan et al., 2006](#)) in FreeSurfer (<http://surfer.nmr.mgh.harvard.edu/fswiki/CorticalParcellation>). Because the main point of the present study was to determine whether changes in cortical metabolism exceed GM atrophy in the earliest, that is, asymptomatic stages of AD, as a conservative approach in the absence of a previously defined cortical thickness template, we selected those brain areas for cortical thickness evaluation that showed a significant decline in the EMCI A β + versus CN A β - subjects and/or LMCI A β + versus CN A β - subjects comparisons. All ROIs are listed in [Table 2](#), in the Section 3.

2.5. Statistical analyses

2.5.1. ROI-based analyses

Individual FDG-uptake values within metabolic ROIs were extracted from the warped FDG-PET maps (before smoothing) by averaging the voxel values within the respective ROI masks in the reference space. The regional FDG-uptake means were converted to SUVRs by normalization to the mean uptake values within the pons mask. Individual GM volumes of the structural ROIs were extracted from the warped GM maps (before smoothing) by summing up the

Table 1
Subjects' characteristics

	CN A β -	CN A β +	EMCI A β +	LMCI A β +
Number of subjects	36	21	65	23
Age	76.1 (± 5.9)	77.7 (± 5.5)	73 (± 6.8) ^a	73.5 (± 8.8)
Age, range	64–89	70–90	62–88	55–87
Gender (male/female)	18/18	12/9	38/27	12/11
Education (y)	16.7 (± 2.6)	16.4 (± 2.5)	15.4 (± 2.7) ^a	16.6 (± 2.6)
MMSE	29 (± 1.1)	28.9 (± 1)	27.8 (± 1.7) ^a	26.9 (± 2.0) ^a
APOE $\epsilon 4$ status (+/-)	7/29	9/12	38/27 ^a	19/4 ^a
Stable status, No. (%)	34 (94.4%)	18 (85.7%)	58 (92.1%) ^b	9 (39.1%) ^a

Key: A β -, β -amyloid negative; A β +, β -amyloid positive; CN, cognitively normal; EMCI, early mild cognitive impairment; LMCI, late mild cognitive impairment; MMSE, Mini Mental State Examination.

^a Indicates a statistically significant difference ($p < 0.05$) with respect to the CN A β - group.

^b Contains 2 subjects without follow-up.

Table 2
ANOVA results of ROI comparisons

ROIs	F (3, 138)	CN Aβ ⁻ versus CN Aβ ⁺ (p)	CN Aβ ⁻ versus EMCI Aβ ⁺ (p)	CN Aβ ⁻ versus LMCI Aβ ⁺ (p)
Glucose metabolic comparisons				
Left inferior parietal	9.464	0.009 ^a	0.104	<0.0005 ^a
	9.598	0.003 ^a		
Medial parietal	8.454	0.008 ^a	0.212	<0.0005 ^a
	7.701	0.008 ^a		
R inferior parietal	7.215	<0.0005 ^a	0.006 ^a	<0.0005 ^a
	16.864	<0.0005 ^a		
Volumetric comparisons				
L lateral temporal	8.338	0.926	0.008 ^a	<0.0005 ^a
L medial temporal	8.890	0.876	0.029 ^a	<0.0005 ^a
R lateral temporal	3.572	0.565	0.011 ^a	0.207
R medial temporal	6.922	0.569	0.016 ^a	<0.0005 ^a
Cortical thickness comparisons				
L banks of superior temporal sulcus	5.530	0.808	0.694	0.001 ^a
L entorhinal cortex	8.853	0.767	0.505	<0.0005 ^a
L fusiform	5.401	0.202	0.057	0.006 ^a
L inferior temporal	5.183	0.220	0.083	<0.0005 ^a
L superior temporal	5.682	0.404	0.370	0.001 ^a
L inferior parietal	6.309	0.113	0.301	0.002 ^a
L isthmus-cingulate	5.920	0.643	0.025 ^a	0.055
R entorhinal cortex	8.288	0.214	0.214	<0.0005 ^a
R fusiform	3.138	0.537	0.067	0.044 ^a
R superior temporal	4.502	0.469	0.151	0.003 ^a

The F values represent the effect of AD stage on ROIs. The *p*-values were calculated in pairwise comparisons among the estimated marginal means. The lower rows in “Glucose metabolic comparisons” report F (1, 51) and *p*-values for the CN Aβ⁺ versus CN Aβ⁻ comparisons in a model including *APOE* ε4 as additional covariate of no interest. Key: Aβ⁻, β-amyloid negative; Aβ⁺, β-amyloid positive; AD, Alzheimer’s disease; ANOVA, analysis of variance; CN, cognitively normal; EMCI, early mild cognitive impairment; L, left; LMCI, late mild cognitive impairment; R, right; ROI, region of interest.

^a Indicates a significant between-group difference (*p* < 0.05). In all statistically significant differences in the table, the estimated marginal means for the CN Aβ⁻ group are larger than the estimated marginal means of the compared group.

modulated GM voxel values within the respective ROI masks. For statistical analysis, the extracted regional GM volumes were normalized by total intracranial volume (TIV). For ROI analysis of the cortical thickness data, average thickness values within the atlas-defined ROIs were calculated automatically as part of the FreeSurfer analysis pipeline. Since cortical thickness has been shown to be independent from head size (Barnes et al., 2010), these ROI values were not normalized by TIV.

Group differences in ROI values were assessed using analysis of covariance, controlling for age, gender, and education, implemented in the Statistics Package for the Social Sciences (SPSS v20.0, Chicago, IL, USA). Statistical significance of the difference in effect size for hypometabolism and atrophy in the asymptomatic AD group (CN Aβ⁺) was assessed using comparison of area under the curve (AUC)-values derived from receiver operating characteristics (ROC) analyses implemented in ROCKIT-software (http://www-radiology.uchicago.edu/krl/KRL_ROC/software_index6.htm) (Metz et al., 1998). Given previous evidence that hypometabolism at asymptomatic stages may rather be mediated by *APOE* ε4 genotype than amyloid status (Jagust and Landau, 2012) we also assessed group differences between CN Aβ⁺ and the CN Aβ⁻ control group controlling for *APOE* ε4 genotype as additional covariate.

2.5.2. Voxel-based analyses

Voxel-based analyses of the imaging data were performed in a series of separate 2-sample *t*-tests in SPM8, comparing each Aβ⁺ group with the CN Aβ⁻ group, controlling for age, gender, and education as confounding variables. Voxel-based analyses of the GM maps were additionally controlled for TIV, calculated as the sum of total volumes of the GM, WM, and CSF partitions. In a separate analysis, group differences between CN Aβ⁺ and CN Aβ⁻ were further controlled for *APOE* ε4 genotype as additional covariate. We did not use *APOE* ε4 as covariate in the analyses of EMCI Aβ⁺ and LMCI Aβ⁺ versus CN Aβ⁻ groups, since these comparisons include an interaction effect of clinical diagnosis by amyloid status,

different from a comparison by amyloid status alone. Preprocessed FDG-PET maps were proportionately scaled to pons uptake values for voxel-based analyses. For both modalities, analyses were restricted to a GM mask of the reference template, thresholded at 20% GM probability, and results were assessed at a statistical threshold of $p_{\text{uncorrected}} < 0.001$ and cluster size $k \geq 50$. In our primary analyses we did not use a conservative multiple comparison correction because we wanted our analyses to be sensitive for effects of atrophy that we had hypothesized to be less pronounced than metabolic effects. Using multiple comparison correction would have inflated the type 2 error to wrongly reject the presence of atrophy. However, voxel-wise results corrected for multiple comparisons are reported in Supplementary Fig. S1. In addition, the Dice coefficient of similarity between the respective maps of hypometabolism and GM atrophy was calculated as an indicator of spatial overlap between the 2 types of neuronal changes.

3. Results

3.1. Demographics and evaluative measures

There were no statistically significant differences in age between CN Aβ⁻ and CN Aβ⁺ subjects ($t[55] = 0.951, p = 0.346$) and between CN Aβ⁻ and LMCI Aβ⁺ subjects ($t[57] = 1.405, p = 0.166$), but there was a significant age difference between CN Aβ⁻ and EMCI Aβ⁺ subjects ($t[99] = 2.369, p = 0.02$). Pearson χ^2 test showed no significant difference in gender distribution among the diagnostic groups ($\chi^2(3, N = 145) = 0.790, p = 0.852$). EMCI Aβ⁺ subjects significantly differed from CN Aβ⁻ subjects in years of education ($U = 860.5, p = 0.026$), but that was not the case with the LMCI Aβ⁺ group ($U = 408.5, p = 0.93$) or with the CN Aβ⁺ group ($U = 351.5, p = 0.655$). In accordance with group definition, EMCI Aβ⁺ subjects and LMCI Aβ⁺ subjects had slightly but significantly lower MMSE scores compared with the CN Aβ⁻ subjects ($U = 647.5, p < 0.001$ and $U = 154.5, p < 0.001$, for EMCI Aβ⁺ and LMCI Aβ⁺, respectively),

whereas MMSE scores of CN A β ⁺ subjects did not significantly differ from CN A β ⁻ subjects ($U = 317$, $p = 0.284$). As expected, frequency of APOE $\epsilon 4$ genotype was significantly higher in the EMCI A β ⁺ ($\chi^2(1) = 14.277$, $p < 0.0005$) and the LMCI A β ⁺ group ($\chi^2(1) = 22.716$, $p < 0.0005$) compared with the CN A β ⁻ control group, and there was a trend for higher APOE $\epsilon 4$ frequency in the CN A β ⁺ group ($\chi^2(1) = 3.601$, $p < 0.06$). Distribution of converters was significantly different only in the LMCI A β ⁺ group ($\chi^2(1) = 20.411$, $p < 0.0005$) in comparison to the distribution of converters in the CN A β ⁻ control group. All tests were 2 tailed. Subjects' characteristics are summarized in Table 1.

3.2. ROI-based findings

Group differences in regional FDG-PET SUVR, TIV-normalized GM volumes, and cortical thickness estimates are summarized in Table 2. A statistically significant main effect of group was found for glucose metabolic reductions in all metabolic ROIs, including left and right inferior parietal and medial parietal cortex. Pairwise comparisons of the estimated marginal means with the CN A β ⁻ control group revealed significant hypometabolism in all 3 ROIs in the CN A β ⁺ group, which also remained significant after controlling for APOE $\epsilon 4$ genotype. Hypometabolism in the EMCI A β ⁺ group was significant for the right inferior parietal ROI, but not for the left inferior parietal and medial parietal ROIs. LMCI A β ⁺ subjects showed highly significant glucose metabolism reductions in all 3 metabolic ROIs.

ROI-based analysis of regional GM volume showed a significant main effect of group for volume reductions in all structural ROIs, including the left and right lateral temporal regions, as well as the left and right medial temporal lobe regions. Pairwise comparisons of the estimated marginal means showed no statistically significant changes in the volume of these regions in CN A β ⁺ subjects compared with CN A β ⁻ subjects. In contrast, the EMCI A β ⁺ group showed significant volume reductions of all 4 ROIs. Volumes in the LMCI A β ⁺ group were also significantly reduced in all but the right lateral temporal ROI.

There were no significant differences in cortical thickness ROIs between CN A β ⁺ subjects and CN A β ⁻ subjects. EMCI A β ⁺ subjects showed significantly reduced thickness in comparison to CN

A β ⁻ subjects in the left isthmus-cingulate region. Significant cortical thinning in LMCI A β ⁺ compared with CN A β ⁻ subjects was observed in the following ROIs: entorhinal cortex, fusiform gyrus and superior temporal region bilaterally as well as inferior temporal gyrus, banks of superior temporal sulcus, and inferior parietal region in the left hemisphere.

Exclusion of the 2 CN A β ⁻ subjects who converted to either MCI or AD dementia, respectively, in a separate set of analyses did not lead to a change in the overall pattern of findings (data not shown).

3.3. ROC analysis results

To determine the significance of the difference between effect sizes for hypometabolism and structural atrophy in the asymptomatic stage of AD, we assessed the potential of the respective ROI measures to distinguish between the CN A β ⁺ group and the CN A β ⁻ control group, as indicated by ROC analyses-derived AUC values. As a first estimate, the AUC value of the metabolic ROI that showed the smallest numerical difference to the CN A β ⁻ control values (left inferior parietal ROI; AUC = 0.765) was compared with the AUC for the left medial temporal lobe region (AUC = 0.540), which was the volumetric ROI that showed the largest numerical difference between the 2 groups (Fig. 1).

The AUC value for the metabolic ROI was significantly higher than the AUC value for the volumetric ROI ($p = 0.008$, 2-tailed). Further comparisons of values of AUCs between other metabolic and volumetric ROIs as well as between the metabolic and cortical thickness ROIs of CN A β ⁺ and CN A β ⁻ subjects also revealed significantly higher hypometabolism than atrophy (data not shown). Thus, the results of ROC analysis indicate that the glucose-uptake metabolic decrease is significantly bigger than the atrophic cortical changes in the asymptomatic AD group.

3.4. Voxel-based findings

In line with the ROI-based findings described previously, voxel-based analysis of preprocessed FDG-PET maps revealed significant hypometabolic areas in CN A β ⁺ compared with CN A β ⁻ subjects, corresponding to medial parietal and bilateral parieto-temporal areas. Additional control for APOE $\epsilon 4$ genotype led to a marked

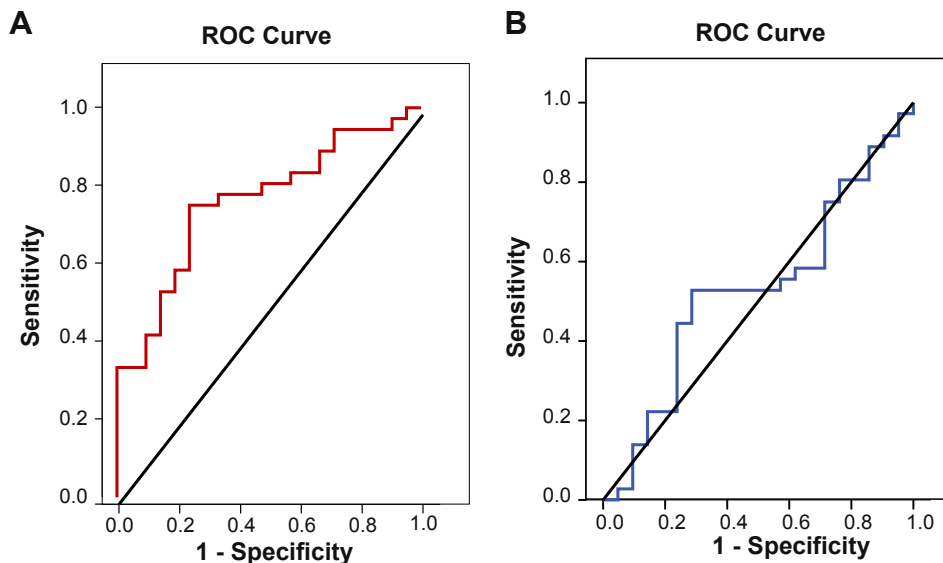


Fig. 1. AUCs for the comparison of the CN A β ⁺ group with the CN A β ⁻ group: (A) hypometabolism in the left inferior parietal region, (B) atrophy in the left medial temporal lobe. Abbreviations: A β , amyloid beta; AUC, area under the curve; CN, cognitively normal.

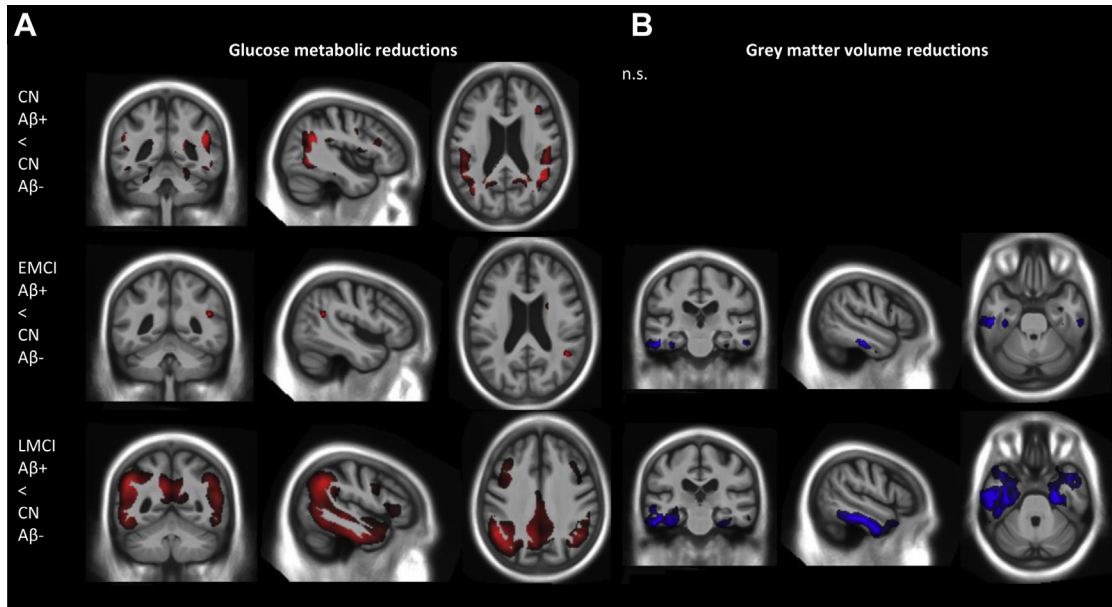


Fig. 2. (A) Hypometabolism (red) and (B) atrophy (blue): results of voxel-based analyses of gray matter maps including age, gender, and education as covariates. The T-maps thresholded at $p_{\text{uncorrected}} < 0.001$ from the SPM voxel-based calculations of the group differences in 2 modalities are overlaid on the study template in MRIcron.

reduction in the extent of hypometabolic areas (Supplementary Fig. S2) and 3 smaller clusters (with 48, 12, and 9 voxels, respectively) of temporoparietal hypometabolism remained significant at $p < 0.05$ FWE-corrected. EMCI Aβ+ subjects exhibited smaller but significant right hemisphere temporoparietal hypometabolism when compared with CN Aβ- subjects. Finally, in LMCI Aβ+ subjects hypometabolism was more extensively distributed across the parietal and temporal lobes and included also parts of the frontal lobe (Fig. 2A).

A voxel-based analysis of GM volume showed no difference between CN Aβ+ and CN Aβ- subjects. However, small clusters of reduced GM volume were found bilaterally in medial and lateral temporal areas in EMCI Aβ+ subjects, whereas LMCI Aβ+ subjects showed marked volume reductions affecting most of the medial temporal areas bilaterally as well as left lateral temporal areas when compared with CN Aβ- controls (Fig. 2B).

The Dice coefficient of similarity assessing the spatial overlap between hypometabolic and GM volumetric changes was 0.10 for the EMCI Aβ+ group and 0.31 for the LMCI Aβ+ group. In the LMCI

group, 76% of the atrophic areas were also hypometabolic, whereas only 19% of the hypometabolic areas were atrophic (Fig. 3).

4. Discussion

Assuming that increased amyloid load initiates a sequence of events leading to AD dementia, in this cross-sectional study we investigated whether hypometabolism exceeds atrophy in amyloid-burdened brains. The main finding of the study is that considerable glucose metabolic reductions appear in the absence of significant cortical or hippocampal atrophy in cognitively normal subjects with increased β-amyloid load. This finding supports the notion that hypometabolism occurs before atrophy in the development of AD.

The results of our study further suggest that hypometabolic and atrophic changes originate in different brain areas. Hypometabolism originates in posterior parieto-temporal areas in asymptomatic amyloid-positive CN subjects. These metabolic alterations are followed by structural changes that first affect medial temporal and lateral temporal areas, as found in the EMCI Aβ+

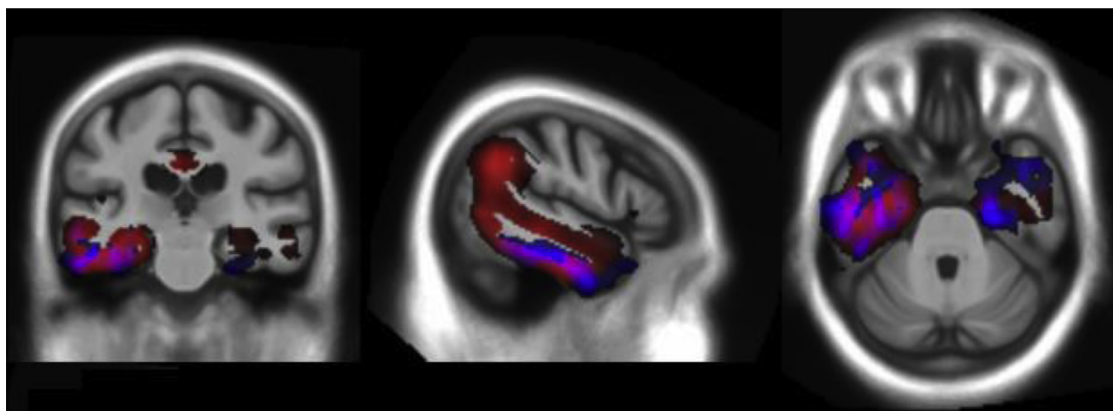


Fig. 3. Patterns of hypometabolism (red) and atrophy (blue) at late MCI stage. The areas of overlap appear as pink. The T-maps thresholded at $p_{\text{uncorrected}} < 0.001$ from the SPM voxel-based calculations of the differences between the LMCI Aβ+ and CN Aβ- groups in each modality are overlaid on the study template in MRIcron. Abbreviations: Aβ, amyloid beta; CN, cognitively normal; LMCI, late mild cognitive impairment; MCI, mild cognitive impairment.

group. In a more advanced predementia stage of disease represented by the LMCI A β + group in the present study both hypometabolism and atrophy spread over large areas, overlapping in the left lateral, and medial temporal regions, and yet retaining their distinct distribution patterns of hypometabolism predominating in the precuneus, posterior parietotemporal, and frontal lobes and atrophy in the medial temporal region (Fig. 3).

When compared with the overall distribution of the widespread hypometabolic changes, the anatomic overlap between atrophy and hypometabolism observed in the LMCI A β + group was in fact not so big, as indicated by a Dice similarity coefficient of 0.3. While most of the atrophic regions in the medial and lateral temporal lobes were also hypometabolic, the hypometabolic pattern was much more widespread and included several regions that did not show evidence of GM atrophy, particularly in the posterior parietal and frontal lobes. Greater hypometabolism than atrophy was also found in patients with mild AD in a range of areas, such as posterior cingulate, precuneus, and inferior parietal areas (Chetelat et al., 2008), which suggests that even though temporal GM atrophy is already prominent at the predementia stage, excessive hypometabolism relative to atrophy appears to continue well into disease.

Apart from our study only a small number of studies so far assessed hypometabolic patterns in amyloid-PET-defined asymptomatic stages of AD, resulting in partly discordant results (Cohen et al., 2009; Drzezga et al., 2011; Jagust and Landau, 2012). Our present findings are at odds with a study by Cohen et al. (2009) who did not find significant hypometabolism in CN A β + when compared with CN A β -. However, our findings agree with a study by Drzezga et al. (2011) who found significant posterior cingulate hypometabolism in a small group of CN A β + when compared with CN A β -, while there was no evidence for AD-related GM atrophy in this group (Drzezga et al., 2011). Another study used the presence of APOE ϵ 4 genotype, as the best-established risk factor for sporadic AD, to model asymptomatic stages of the disease, and found significant posterior parietal hypometabolism in the absence of hippocampal atrophy when compared with healthy controls without this risk factor (Protas et al., 2013). APOE ϵ 4 genotype and other hitherto unknown genetic risk factors conveyed by a family history of sporadic AD are highly correlated with increased cortical amyloid deposition (Morris et al., 2010; Mosconi et al., 2010; Reiman et al., 2009), and their presence in cognitively normal subjects has been used in other studies to model asymptomatic stages of sporadic AD. Thus, cognitively healthy subjects at genetic risk for AD and particularly carriers of the APOE ϵ 4 allele were found to show increased amyloid load and hypometabolism in AD-susceptible areas (Mosconi et al., 2013; Reiman et al., 2001), but not hippocampal atrophy (Protas et al., 2013) when compared with healthy controls without these genetic risk factors.

Using a different subset of ADNI data than the one used in the present study, Jagust and Landau (2012) aimed to disentangle the effects of amyloid status and APOE ϵ 4 genotype on cortical hypometabolism at asymptomatic stages and found that amyloid status had no additional effect on cortical metabolism that was not already explained by APOE ϵ 4 genotype (Jagust and Landau, 2012). The present study used PET-measured amyloid positivity as defining criterion for the asymptomatic AD stage, as suggested by recently revised research criteria (Sperling et al., 2011), to assess the differential expression of atrophy and hypometabolism at this presumably earliest stage of AD development. While disentangling the precise genetic-molecular origins of hypometabolism at the asymptomatic stage of AD was not the primary aim of the present study, we additionally controlled the comparison between CN A β + and CN A β - for APOE ϵ 4 genotype to assess the specificity of the effects for amyloid status. Interestingly, and in contrast to the

findings by Jagust and Landau (2012), regional hypometabolism in the CN A β + group remained significant, albeit markedly reduced in extent, when controlling for APOE ϵ 4 genotype. These differential findings between the studies are not likely to be primarily because of methodical issues, given that Jagust and Landau (2012) used similarly sensitive ROI-based analyses complemented by voxel-based explorations. Rather, the asymptomatic stage of AD as defined by CN A β + individuals may be very heterogeneous with regard to cortical hypometabolism, depending on how much, on average, the included individuals have already progressed further down the pathologic cascade. Thus, there is accumulating evidence from both autosomal dominant AD (Benzinger et al., 2013) and sporadic AD (O'Brien et al., 2010) that neuronal activity and metabolism may even show transient increases at very early asymptomatic stages, which are followed by steady decreases as the disease evolves. Given the high collinearity of APOE ϵ 4 genotype and amyloid-status at asymptomatic stages (Morris et al., 2010), separate effects of these predictors are not easily disentangled in statistical models and may yield mixed results dependent on slightly differing sample characteristics. Further elucidation of the interplay of amyloid burden and APOE ϵ 4 genotype in the development of AD-related neuronal injury is needed.

Our finding that hypometabolism exceeds atrophy at the presumably earliest stage of AD development has implications for a combined model of AD that seeks to explain both autosomal dominantly inherited and sporadic types of AD. The model postulates that the order of events in a sequence leading to AD dementia may be the same in autosomal dominant AD and sporadic AD (Bateman et al., 2012). An early study including 7 autosomal dominant AD and 7 age-, gender-, and education-matched healthy subjects showed significant hypometabolism without marked GM atrophy in these patients (Mosconi et al., 2006). However, Bateman et al. (2012) investigated clinical and biomarker changes in 128 autosomal dominant AD participants of the Dominantly Inherited Alzheimer Network and found that in mutation carriers an excessive amyloid load in the precuneus was followed by bilateral hippocampal atrophy approximately 15 years before the expected symptom onset, whereas hypometabolism in the precuneus was first observed 10 years before the expected symptom onset. More recent Dominantly Inherited Alzheimer Network findings based on an extended cohort ($n = 229$) confirmed that significant hypometabolism in the precuneus and/or posterior cingulate and lateral parietal cortex can be detected 10 years before the estimated age of onset. However, hippocampus atrophy got significant at approximately the same time, and regional cortical atrophy was not observed until 5 years before the estimated age of onset (Benzinger et al., 2013). Beside possible differences in the pathologic trajectories between autosomal dominant and sporadic AD, the discrepancy with our present findings of posterior parietal hypometabolism in the absence of hippocampal and/or medial temporal atrophy at the asymptomatic stage of AD may also be because of methodical differences. Thus, differing analysis approaches and applied statistical thresholds used for assessment of cortical hypometabolism and hippocampal atrophy in the study by Benzing et al. (2013) could have led to a higher sensitivity for detection of hippocampal atrophy compared with cortical hypometabolism. Using longitudinal data from cognitively normal and predemented individuals, Villemagne et al. (2013) recently estimated the time when hippocampal atrophy becomes significant in sporadic AD to be approximately 5 years before the onset of dementia, most likely coinciding with the predementia stage of AD (Villemagne et al., 2013). Regarding the relative degrees of atrophy and hypometabolism at asymptomatic disease stages, Ewers et al. (2013) recently found that temporoparietal hypometabolism but not medial temporal lobe atrophy, significantly predicted clinical

decline to MCI or AD in initially cognitively normal individuals (Ewers et al., 2013).

There are some limitations to the present study. First, the study is cross-sectional and the stages of AD represented by the CN A β +, EMCI A β +, and LMCI A β + groups do not capture individual longitudinal changes. The presence of AD pathology in these subjects was inferred from PET-imaging evidence of abnormal levels of cortical amyloid deposits, whereas the presence and severity of memory deficits were used to stage these amyloid-positive individuals into preclinical as well as early and late predementia groups of AD. Although this approach is consistent with the recently revised diagnostic criteria for AD in research settings (Albert et al., 2011; Dubois et al., 2007; Sperling et al., 2011), at this point it still remains hypothetical if all these subjects will eventually develop AD dementia. In addition, given the degree of heterogeneity observed in the preclinical AD stage with regard to hypometabolism, hippocampal atrophy, and subclinical cognitive impairments (Jack et al., 2012), the grouping of subjects in our study may have resulted in only a partial insight into the issues addressed. Thus, the patterns of hypometabolism and atrophy that we observed in asymptomatic and predementia AD stages should be interpreted with these caveats in mind. Another possible limitation of the study pertains to the cortical thickness ROIs. These were derived from the atrophic and hypometabolic effects found in the predementia stages of our own study's sample, which might have led to an overestimation of cortical thickness reductions in CN A β + versus CN A β - subjects when comparing metabolic and structural changes. However, regardless of the possible overestimation of cortical thinning effects in the CN A β + group, ROC analyses also demonstrated higher effect sizes for hypometabolism compared with cortical thickness changes in these subjects.

In conclusion, the results of the present cross-sectional study support a temporal ordering of neuronal injury markers in sporadic AD, according to which hypometabolism generally precedes atrophy, although with partly differing regional manifestations (Jack et al., 2010). The study provides a framework for the testing of assumptions on disease pathogenesis using *in vivo* imaging markers and for comparison of a proposed sequence of pathologic events between sporadic and genetically determined cases of preclinical and predementia AD. Future studies will investigate the longitudinal course of hypometabolism and atrophy in cognitively unimpaired and mildly impaired subjects stratified according to their amyloid status.

Disclosure statement

There are no actual or potential conflicts of interest.

Acknowledgements

Data collection and sharing for this project was funded by the Alzheimer's Disease Neuroimaging Initiative (ADNI) (National Institutes of Health Grant U01 AG024904). ADNI is funded by the National Institute on Aging, the National Institute of Biomedical Imaging and Bioengineering, and through generous contributions from the following: Abbott; Alzheimer's Association; Alzheimer's Drug Discovery Foundation; Amorfix Life Sciences Ltd; AstraZeneca; Bayer HealthCare; BioClinica, Inc; Biogen Idec Inc; Bristol-Myers Squibb Company; Eisai Inc; Elan Pharmaceuticals Inc; Eli Lilly and Company; F. Hoffmann-La Roche Ltd and its affiliated company Genentech, Inc; GE Healthcare; Innogenetics, N.V.; IXICO Ltd; Janssen Alzheimer Immunotherapy Research & Development, LLC.; Johnson & Johnson Pharmaceutical Research & Development LLC.; Medpace, Inc; Merck & Co, Inc; Meso Scale Diagnostics, LLC.; Novartis Pharmaceuticals Corporation; Pfizer Inc; Servier; Synarc

Inc; and Takeda Pharmaceutical Company. The Canadian Institutes of Health Research is providing funds to support ADNI clinical sites in Canada. Private Rev November 7, 2012 sector contributions are facilitated by the Foundation for the National Institutes of Health (www.fnih.org). The grantee organization is the Northern California Institute for Research and Education, and the study is coordinated by the Alzheimer's Disease Cooperative Study at the University of California, San Diego. ADNI data are disseminated by the Laboratory for Neuro Imaging at the University of California, Los Angeles. This research was also supported by NIH grants P30 AG010129 and K01 AG030514. The authors thank Florian Bauer for preprocessing the cortical thickness data, Christina Schuster and Martin Dyrba for their help with FreeSurfer, and Christoph Berger for a discussion on ROI analyses. They are grateful to 3 anonymous reviewers for their helpful comments and suggestions.

Appendix A. Supplementary data

Supplementary data associated with this article can be found, in the online version, at <http://dx.doi.org/10.1016/j.neurobiolaging.2014.04.006>.

References

- Albert, M.S., DeKosky, S.T., Dickson, D., Dubois, B., Feldman, H.H., Fox, N.C., Gamst, A., Holtzman, D.M., Jagust, W.J., Petersen, R.C., Snyder, P.J., Carrillo, M.C., Thies, B., Phelps, C.H., 2011. The diagnosis of mild cognitive impairment due to Alzheimer's disease: recommendations from the National Institute on Aging-Alzheimer's Association workgroups on diagnostic guidelines for Alzheimer's disease. *Alzheimers Dement.* 7, 270–279.
- Ashburner, J., 2007. A fast diffeomorphic image registration algorithm. *Neuroimage* 38, 95–113.
- Barnes, J., Ridgway, G.R., Bartlett, J., Henley, S.M., Lehmann, M., Hobbs, N., Clarkson, M.J., MacManus, D.G., Ourselin, S., Fox, N.C., 2010. Head size, age and gender adjustment in MRI studies: a necessary nuisance? *Neuroimage* 53, 1244–1255.
- Bateman, R.J., Xiong, C., Benzinger, T.L., Fagan, A.M., Goate, A., Fox, N.C., Marcus, D.S., Cairns, N.J., Xie, X., Blazey, T.M., Holtzman, D.M., Santacruz, A., Buckles, V., Oliver, A., Moulder, K., Aisen, P.S., Ghetti, B., Klunk, W.E., McDade, E., Martins, R.N., Masters, C.L., Mayeux, R., Ringman, J.M., Rossor, M.N., Schofield, P.R., Sperling, R.A., Salloway, S., Morris, J.C., 2012. Clinical and biomarker changes in dominantly inherited Alzheimer's disease. *New Engl. J. Med.* 367, 795–804.
- Benzinger, T.L., Blazey, T., Jack Jr., C.R., Koeppe, R.A., Su, Y., Xiong, C., Raichle, M.E., Snyder, A.Z., Ances, B.M., Bateman, R.J., Cairns, N.J., Fagan, A.M., Goate, A., Marcus, D.S., Aisen, P.S., Christensen, J.J., Ercole, L., Hornbeck, R.C., Farrar, A.M., Aldea, P., Jasielec, M.S., Owen, C.J., Xie, X., Mayeux, R., Brickman, A., McDade, E., Klunk, W., Mathis, C.A., Ringman, J., Thompson, P.M., Ghetti, B., Saykin, A.J., Sperling, R.A., Johnson, K.A., Salloway, S., Correia, S., Schofield, P.R., Masters, C.L., Rowe, C., Villemagne, V.L., Martins, R., Ourselin, S., Rossor, M.N., Fox, N.C., Cash, D.M., Weiner, M.W., Holtzman, D.M., Buckles, V.D., Moulder, K., Morris, J.C., 2013. Regional variability of imaging biomarkers in autosomal dominant Alzheimer's disease. *Proc. Natl. Acad. Sci. USA* 110, E4502–E4509.
- Buchhave, P., Minthon, L., Zetterberg, H., Wallin, A.K., Blennow, K., Hansson, O., 2012. Cerebrospinal fluid levels of beta-amyloid 1–42, but not of tau, are fully changed already 5 to 10 years before the onset of Alzheimer dementia. *Arch. Gen. Psychiatry* 69, 98–106.
- Castellani, R.J., Smith, M.A., 2011. Compounding artefacts with uncertainty, and an amyloid cascade hypothesis that is 'too big to fail'. *J. Pathol.* 224, 147–152.
- Chetelat, G., Desgranges, B., Landeau, B., Mezenge, F., Poline, J.B., Sayette, V., Viader, F., Eustache, F., Baron, J.-C., 2008. Direct voxel-based comparison between grey matter hypometabolism and atrophy in Alzheimer's disease. *Brain* 131, 60–71.
- Cohen, A.D., Price, J.C., Weissfeld, L.A., James, J., Rosario, B.L., Bi, W., Nebes, R.D., Saxton, J.A., Snitz, B.E., Aizenstein, H.A., Wolk, D.A., Dekosky, S.T., Mathis, C.A., Klunk, W.E., 2009. Basal cerebral metabolism may modulate the cognitive effects of A β in mild cognitive impairment: an example of brain reserve. *J. Neurosci.* 29, 14770–14778.
- Dale, A.M., Fischl, B., Sereno, M.I., 1999. Cortical surface-based analysis. I. Segmentation and surface reconstruction. *Neuroimage* 9, 179–194.
- Desikan, R.S., Sponne, F., Fischl, B., Quinn, B.T., Dickerson, B.C., Blacker, D., Buckner, R.L., Dale, A.M., Maguire, R.P., Hyman, B.T., Albert, M.S., Killiany, R.J., 2006. An automated labeling system for subdividing the human cerebral cortex on MRI scans into gyral based regions of interest. *Neuroimage* 31, 968–980.
- Dickerson, B.C., Bakkour, A., Salat, D.H., Feczko, E., Pacheco, J., Greve, D.N., Grotstein, F., Wright, C.I., Blacker, D., Rosas, H.D., Sperling, R.A., Atri, A., Growdon, J.H., Hyman, B.T., Morris, J.C., Fischl, B., Buckner, R.L., 2009. The cortical signature of Alzheimer's disease: regionally specific cortical thinning

- relates to symptom severity in very mild to mild AD dementia and is detectable in asymptomatic amyloid-positive individuals. *Cereb. Cortex* 19, 497–510.
- Drzezga, A., Becker, J.A., Van Dijk, K.R., Sreenivasan, A., Talukdar, T., Sullivan, C., Schultz, A.P., Sepulcre, J., Putcha, D., Greve, D., Johnson, K.A., Sperling, R.A., 2011. Neuronal dysfunction and disconnection of cortical hubs in non-demented subjects with elevated amyloid burden. *Brain* 134, 1635–1646.
- Dubois, B., Feldman, H.H., Jacova, C., Cummings, J.L., Dekosky, S.T., Barberger-Gateau, P., Delacourte, A., Frisoni, G., Fox, N.C., Galasko, D., Gauthier, S., Hampel, H., Jicha, G.A., Meguro, K., O'Brien, J., Pasquier, F., Robert, P., Rossor, M., Salloway, S., Sarazin, M., de Souza, L.C., Stern, Y., Visser, P.J., Scheltens, P., 2010. Revising the definition of Alzheimer's disease: a new lexicon. *Lancet Neurol.* 9, 1118–1127.
- Dubois, B., Feldman, H.H., Jacova, C., Dekosky, S.T., Barberger-Gateau, P., Cummings, J., Delacourte, A., Galasko, D., Gauthier, S., Jicha, G., Meguro, K., O'Brien, J., Pasquier, F., Robert, P., Rossor, M., Salloway, S., Stern, Y., Visser, P.J., Scheltens, P., 2007. Research criteria for the diagnosis of Alzheimer's disease: revising the NINCDS-ADRDA criteria. *Lancet Neurol.* 6, 734–746.
- Ewers, M., Brendel, M., Rizk-Jackson, A., Rominger, A., Bartenstein, P., Schuff, N., Weiner, M.W., 2013. Reduced FDG-PET brain metabolism and executive function predict clinical progression in elderly healthy subjects. *Neuroimage Clin.* 4, 45–52.
- Fischl, B., Sereno, M.I., Dale, A.M., 1999. Cortical surface-based analysis. II: inflation, flattening, and a surface-based coordinate system. *Neuroimage* 9, 195–207.
- Glenner, G.G., Wong, C.W., 1984. Alzheimer's disease: initial report of the purification and characterization of a novel cerebrovascular amyloid protein. *Biochem. Biophys. Res. Commun.* 120, 885–890.
- Grothe, M., Heinsen, H., Teipel, S., 2013. Longitudinal measures of cholinergic forebrain atrophy in the transition from healthy aging to Alzheimer's disease. *Neurobiol. Aging* 34, 1210–1220.
- Hardy, J., Allsop, D., 1991. Amyloid deposition as the central event in the aetiology of Alzheimer's disease. *Trends Pharmacol. Sci.* 12, 383–388.
- Hardy, J.A., Higgins, G.A., 1992. Alzheimer's disease: the amyloid cascade hypothesis. *Science* 256, 184–185.
- Jack Jr., C.R., Knopman, D.S., Jagust, W.J., Petersen, R.C., Weiner, M.W., Aisen, P.S., Shaw, L.M., Vemuri, P., Wiste, H.J., Weigand, S.D., Lesnick, T.G., Pankratz, V.S., Donohue, M.C., Trojanowski, J.Q., 2013. Tracking pathophysiological processes in Alzheimer's disease: an updated hypothetical model of dynamic biomarkers. *Lancet Neurol.* 12, 207–216.
- Jack Jr., C.R., Knopman, D.S., Jagust, W.J., Shaw, L.M., Aisen, P.S., Weiner, M.W., Petersen, R.C., Trojanowski, J.Q., 2010. Hypothetical model of dynamic biomarkers of the Alzheimer's pathological cascade. *Lancet Neurol.* 9, 119–128.
- Jack Jr., C.R., Knopman, D.S., Weigand, S.D., Wiste, H.J., Vemuri, P., Lowe, V., Kantarci, K., Gunter, J.L., Senjem, M.L., Ivnik, R.J., Roberts, R.O., Rocca, W.A., Boeve, B.F., Petersen, R.C., 2012. An operational approach to National Institute on Aging-Alzheimer's Association criteria for preclinical Alzheimer disease. *Ann. Neurol.* 71, 765–775.
- Jagust, W.J., Landau, S.M., 2012. Apolipoprotein E, not fibrillar beta-amyloid, reduces cerebral glucose metabolism in normal aging. *J. Neurosci.* 32, 18227–18233.
- Jagust, W.J., Landau, S.M., Shaw, L.M., Trojanowski, J.Q., Koeppe, R.A., Reiman, E.M., Foster, N.L., Petersen, R.C., Weiner, M.W., Price, J.C., Mathis, C.A., 2009. Relationships between biomarkers in aging and dementia. *Neurology* 73, 1193–1199.
- Karran, E., Mercken, M., De Strooper, B., 2011. The amyloid cascade hypothesis for Alzheimer's disease: an appraisal for the development of therapeutics. *Nat. Rev.* 10, 698–712.
- Khachaturian, A.S., Mielke, M.M., Khachaturian, Z.S., 2012. Biomarker development: a population-level perspective. *Alzheimers Dement.* 8, 247–249.
- Lee, H.G., Casadesus, G., Zhu, X., Takeda, A., Perry, G., Smith, M.A., 2004. Challenging the amyloid cascade hypothesis: senile plaques and amyloid-beta as protective adaptations to Alzheimer disease. *Ann. N.Y. Acad. Sci.* 1019, 1–4.
- Metz, C.E., Herman, B.A., Roe, C.A., 1998. Statistical comparison of two ROC-curve estimates obtained from partially-paired datasets. *Med. Decis. Making* 18, 110–121.
- Mormino, E.C., Kluth, J.T., Madison, C.M., Rabinovici, G.D., Baker, S.L., Miller, B.L., Koeppe, R.A., Mathis, C.A., Weiner, M.W., Jagust, W.J., 2009. Episodic memory loss is related to hippocampal-mediated -amyloid deposition in elderly subjects. *Brain* 132, 1310–1323.
- Morris, J.C., Roe, C.M., Xiong, C., Fagan, A.M., Goate, A.M., Holtzman, D.M., Mintun, M.A., 2010. APOE predicts amyloid-beta but not tau Alzheimer pathology in cognitively normal aging. *Ann. Neurol.* 67, 122–131.
- Mosconi, L., 2005. Brain glucose metabolism in the early and specific diagnosis of Alzheimer's disease. *FDG-PET studies in MCI and AD. Eur. J. Nucl. Med. Mol. Imaging* 32, 486–510.
- Mosconi, L., Rinne, J.O., Tsui, W.H., Berti, V., Li, Y., Wang, H., Murray, J., Scheinin, N., Nägren, K., Williams, S., Glodzik, L., De Santi, S., Vallabhajosula, S., de Leon, M.J., 2010. Increased fibrillar amyloid- β burden in normal individuals with a family history of late-onset Alzheimer's. *Proc. Natl. Acad. Sci. U.S.A.* 107, 5949–5954.
- Mosconi, L., Rinne, J.O., Tsui, W.H., Murray, J., Li, Y., Glodzik, L., McHugh, P., Williams, S., Cummings, M., Pirraglia, E., Goldsmith, S.J., Vallabhajosula, S., Scheinin, N., Viljanen, T., Nägren, K., de Leon, M.J., 2013. Amyloid and metabolic positron emission tomography imaging of cognitively normal adults with Alzheimer's parents. *Neurobiol. Aging* 34, 22–34.
- Mosconi, L., Sorbi, S., de Leon, M.J., Li, Y., Nacmias, B., Myoung, P.S., Tsui, W., Ginestroni, A., Bessi, V., Fayyaz, M., Caffarra, P., Pupi, A., 2006. Hypometabolism exceeds atrophy in presymptomatic early-onset familial Alzheimer's disease. *J. Nucl. Med.* 47, 1778–1786.
- Nordberg, A., Carter, S.F., Rinne, J., Drzezga, A., Brooks, D.J., Vandenberghe, R., Perani, D., Forsberg, A., Långström, B., Scheinin, N., Karrasch, M., Nägren, K., Grimmer, T., Miederer, I., Edison, P., Okello, A., Van Laere, K., Nelissen, N., Vandenberghe, M., Garibotto, V., Almkvist, O., Kalbe, E., Hinz, R., Herholz, K., 2013. A European multicentre PET study of fibrillar amyloid in Alzheimer's disease. *Eur. J. Nucl. Med. Mol. Imaging* 40, 104–114.
- O'Brien, J.L., O'Keefe, K.M., LaViolette, P.S., DeLuca, A.N., Blacker, D., Dickerson, B.C., Sperling, R.A., 2010. Longitudinal fMRI in elderly reveals loss of hippocampal activation with clinical decline. *Neurology* 74, 1969–1976.
- Ossenkoppele, R., van Berckel, B.N., Prins, N.D., 2011. Amyloid imaging in prodromal Alzheimer's disease. *Alzheimers Res. Ther.* 3, 26.
- Pimplikar, S.W., 2009. Reassessing the amyloid cascade hypothesis of Alzheimer's disease. *Int. J. Biochem. Cell Biol* 41, 1261–1268.
- Protas, H.D., Chen, K., Langbaum, J.B., Fleisher, A.S., Alexander, G.E., Lee, W., Bandy, D., de Leon, M.J., Mosconi, L., Buckley, S., Truran-Sacrey, D., Schuff, N., Weiner, M.W., Caselli, R.J., Reiman, E.M., 2013. Posterior cingulate glucose metabolism, hippocampal glucose metabolism, and hippocampal volume in cognitively normal, late-middle-aged persons at 3 levels of genetic risk for Alzheimer disease. *JAMA Neurol.* 70, 320–325.
- Reiman, E.M., Caselli, R.J., Chen, K., Alexander, G.E., Bandy, D., Frost, J., 2001. Declining brain activity in cognitively normal apolipoprotein E epsilon 4 heterozygotes: a foundation for using positron emission tomography to efficiently test treatments to prevent Alzheimer's disease. *Proc. Natl. Acad. Sci. U.S.A.* 98, 3334–3339.
- Reiman, E.M., Chen, K., Liu, X., Bandy, D., Yu, M., Lee, W., Ayutyanont, N., Keppler, J., Reeder, S.A., Langbaum, J.B., Alexander, G.E., Klunk, W.E., Mathis, C.A., Price, J.C., Aizenstein, H.J., DeKosky, S.T., Caselli, R.J., 2009. Fibrillar amyloid-beta burden in cognitively normal people at 3 levels of genetic risk for Alzheimer's disease. *Proc. Natl. Acad. Sci. U.S.A.* 106, 6820–6825.
- Sperling, R.A., Aisen, P.S., Beckett, L.A., Bennett, D.A., Craft, S., Fagan, A.M., Iwatsubo, T., Jack Jr., C.R., Kaye, J., Montine, T.J., Park, D.C., Reiman, E.M., Rowe, C.C., Siemers, E., Stern, Y., Yaffe, K., Carrillo, M.C., Thies, B., Morrison-Bogorad, M., Wagster, M.V., Phelps, C.H., 2011. Toward defining the preclinical stages of Alzheimer's disease: recommendations from the National Institute on Aging-Alzheimer's Association workgroups on diagnostic guidelines for Alzheimer's disease. *Alzheimers Dement.* 7, 280–292.
- Villemagne, V.L., Burnham, S., Bourgeat, P., Brown, B., Ellis, K.A., Salvado, O., Szeke, C., Macaulay, S.L., Martins, R., Maruff, P., Ames, D., Rowe, C.C., Masters, C.L., 2013. Amyloid beta deposition, neurodegeneration, and cognitive decline in sporadic Alzheimer's disease: a prospective cohort study. *Lancet Neurol.* 12, 357–367.